

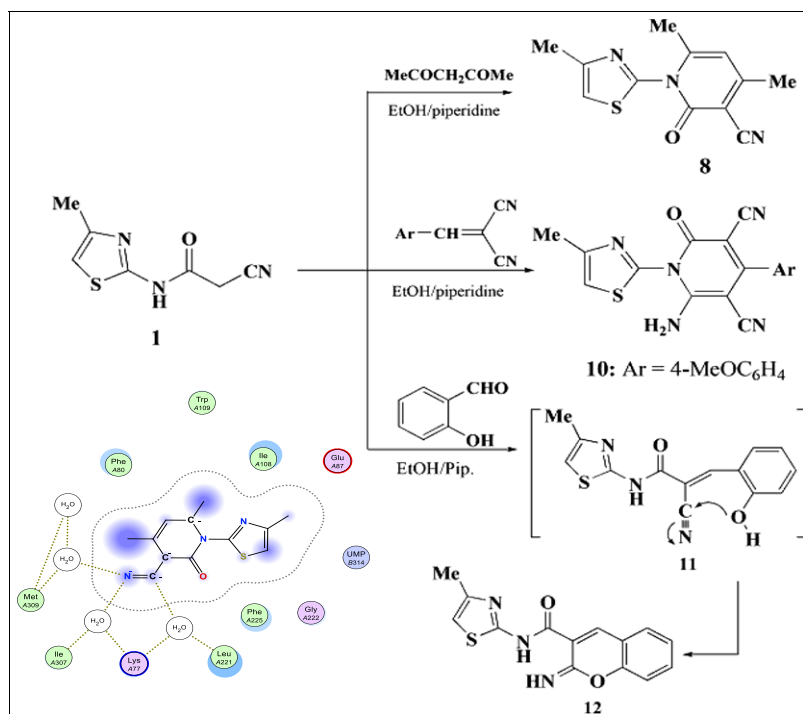
^aDepartment of Chemistry, Turabah University College, Taif University, Taif 21995, Saudi Arabia
^bChemistry Department, Faculty of Science, University of Khartoum, Khartoum P.O. Box 321, Sudan

*E-mail: a_radwan2000@yahoo.com; a.radwan@tu.edu.sa

Received September 23, 2018

DOI 10.1002/jhet.3493

Published online 00 Month 2019 in Wiley Online Library (wileyonlinelibrary.com).



2-Cyanoacetamido-4-methylthiazole (**1**) was utilized as a versatile precursor for the construction of new thiazole clubbed thiazolidine, thiophene, pyridine, or chromene scaffold. The base-catalyzed addition of **1** to phenyl isothiocyanate followed by subsequent treatment of the produced thiocarbamoyl intermediate with ethyl chloroacetate or chloroacetonitrile furnished the corresponding thiazolyl-thiazolidine and thiazolyl-thiophene hybrids. The reactions of compound **1** with chemical reagents, namely, acetylacetone, malononitrile, and/or 2-(4-anisylidene)-malononitrile have been studied and furnished the corresponding thiazole-pyridine hydrides **8–10**. Furthermore, treatment of the precursor **1** with salicylaldehyde, various aryl diazonium chlorides, and/or aromatic aldehydes afforded their corresponding thiazolyl-chromene hybrid **12**, arylhydrazono-nitriles **13**, and unsaturated nitriles **14**, respectively. The cytotoxicity of the synthesized compounds was screened against the cell lines HepG2, HCT-116, and MCF-7. Compounds **8**, **10**, and **12** recorded the best results, which was illustrated by molecular docking. Molecular Operating Environment molecular docking calculations carried out here is to rationalize correlation between docking results and biological data of thymidylate synthase (Protein Data Bank code: IHVY) inhibition. Docking has been carried out in the same co-crystallographic inhibitor binding site to predict if the binding mode of active compounds is analogous to that of native inhibitor.

J. Heterocyclic Chem., **00**, 00 (2019).

INTRODUCTION

Thiazole-containing heterocycles are important class of compounds that have a wide range of biological activities [1]. They are well established to possess antimicrobial [2], anti-inflammatory [3], antitubercular [4,5], anticonvulsant [6,7], and anticancer [8–11] activities. Aminothiazole-containing medicines have been applied in

clinical use for over 30 years, for example, famotidine is used for the treatment of peptic ulcer and controls gastro esophageal reflux [12], and proved to be nine times more potent than ranitidine [13]; Abafungin as antifungal agent is used in the treatment of dermatomycoses [14], and Cefdinir is well-known FDA-approved antibiotic and a third generation broad spectrum cephalosporin [15]. Recently, some new thiazoles have been synthesized and

proved to possess antioxidant property and DNA damage inhibition ability [16,17]. The biological and synthetic significance of thiazole-containing heterocycles prompted us to design and synthesize new thiazole clubbed thiazolidine, thiophene, pyridine, or chromene derivatives to screen its activity as anticancer.

The enzyme thymidylate synthase (TS) is very important in the synthesis of 2'-deoxythymidine-5'-monophosphate, which consider to be quite essential in DNA biosynthesis [18–20], and this explain why this enzyme is attracted so many researchers in the field of cancer chemotherapy [19].

The most prominent inhibitor for TS is 5-fluorouracil, which have been used widely for the treatment of breast, ovarian, pancreatic, head, neck, gastric, and colorectal cancers [21]. Schmitz and his co-authors found that the activity of 5-fluorouracil in colorectal cancer treatment can be enhanced by the addition of leucovorin and reduced folate, and the response rates of these combinations remain in the range 25–30%; this finding leads to put much efforts that focused on designing new and more potent TS inhibitors [21]. Raltitrexed, as a folate analogue inhibitor, is used widely in Australia, Japan, Canada, and Europe as first-line therapy for treatment of colorectal cancer, although is considered to be under investigation in the United States. For now, so many TS inhibitors are available for general clinical treatment; further researches are needed to connect between the critical biochemical and molecular factors that determine the tumor specificity and efficacy of each compound.

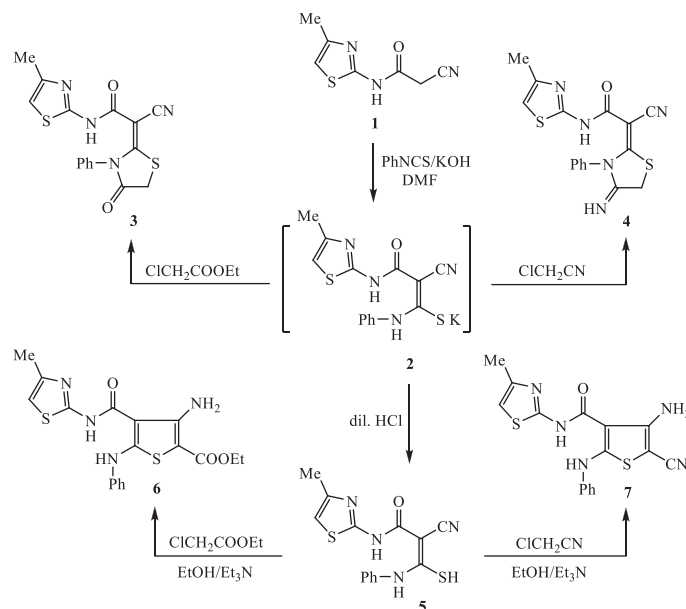
The most intuitive and effective research method used to study the binding between target proteins and drug molecules is the molecular docking, and recently, this method gets more attention from researchers worldwide; it is easy with this method to reveal insight information about the mechanism of interaction between target proteins and drug molecules as well as the conformational change of the resulted complex from different aspects. In this study, series of active new compounds were prepared and presented using a direct synthesis approach, and the interaction mode between the synthesized compounds and TS active site was demonstrated by molecular modeling techniques using Molecular Operating Environment (MOE) software.

RESULTS AND DISCUSSION

Chemistry. The key 4-methyl-2-thiazolyl-cyanoacetamide (**1**) has been synthesized by heating 2-amino-4-methylthiazole with cyanoacetic acid in the presence of acetic anhydride according to the previously published procedure [22]. Treatment of 4-methyl-2-thiazolyl-cyanoacetamide (**1**) with equimolar amount of phenyl isothiocyanate in dimethylformamide (DMF)

containing potassium hydroxide furnished the non-isolable intermediate potassium sulfide salt **2**, which underwent *in situ* addition of ethyl chloroacetate at room temperature to afford 2-cyano-2-(4-oxo-3-phenylthiazolidin-2-ylidene)-*N*-(4-methylthiazol-2-yl)acetamide (**3**) (Scheme 1). The chemical structure of this thiazolidinone was established based on its spectral and elemental analyses. Infrared spectrum of thiazolidinone derivative **3** showed the characteristic absorption bands at wave numbers 3127, 2199, and 1740 cm^{-1} to indicate the presence of the functional groups NH of amide, cyano, and carbonyl of the thiazolidine ring, respectively. The singlet signal for two protons at δ 4.04 ppm ($^1\text{H-NMR}$ spectrum), clearly indicated the presence of methylene group of the thiazolidinone ring. The *in situ* addition of chloroacetonitrile to potassium salt **2** proceeded at room temperature afforded 2-cyano-2-(4-imino-3-phenylthiazolidin-2-ylidene)-*N*-(4-methylthiazol-2-yl)acetamide (**4**). The chemical structure of this product was assured from its spectral and elemental analyses. Its IR spectrum clearly displayed characteristic absorption bands at wave numbers 3346, 2194, and 1664 cm^{-1} that refer to N–H of amide, cyano, and carbonyl functions, respectively. The singlet signal for two protons at δ 3.92 ppm ($^1\text{H-NMR}$ spectrum) clearly indicated the presence of methylene group of the thiazolidine ring.

2-Cyano-3-mercapto-3-(phenylamino)-*N*-(4-methylthiazol-2-yl)acrylamide (**5**) has been achieved *via* treatment of **1** with phenyl isothiocyanate in DMF as a solvent and potassium hydroxide as a catalyst, followed by neutralization with dilute hydrochloric acid (Scheme 1). Different behavior, rather than the formation of thiazole derivatives, was observed when thiocarbamoyl scaffold **5** was allowed to react with α -halogenated reagents in ethanol containing catalytic amount of Et_3N . The reaction of compound **5** with ethyl chloroacetate in hot ethyl alcohol containing drops of triethyl amine furnished ethyl 4-(4-methylthiazol-2-ylcarbonyl)-3-amino-5-(phenylamino)-thiophene-2-carboxylate (**6**). In addition, heterocyclization of compound **5** with chloroacetonitrile by reflux in ethyl alcohol containing drops of triethyl amine furnished the corresponding 4-amino-5-cyano-2-(phenylamino)-*N*-(4-methylthiazol-2-yl)thiophene-3-carboxamide (**7**). Various spectral techniques were utilized to secure the suggested chemical structures of these newly synthesized thiophene scaffolds. For example, IR spectrum of thiophene derivative **6** exhibited absorption bands at wave numbers 3416 and 3243 cm^{-1} and 1638 cm^{-1} for the N-H stretch vibrations (NH_2 and NH) and carbonyl functions, respectively. $^1\text{H-NMR}$ spectrum of the same thiophene scaffold **6** displayed triplet signals at δ 1.31 ppm and quartet signal at δ 4.30 ppm for the ethyl of ester ($\text{COOCH}_2\text{CH}_3$), singlet for three protons at δ 2.11 ppm (CH_3), singlet signal for two protons at δ 6.90 ppm (NH_2),

Scheme 1. Reactions of thiazolyl-cyanoacetamide **1** with phenyl isothiocyanate/ethyl chloroacetate and/or chloroacetonitrile.

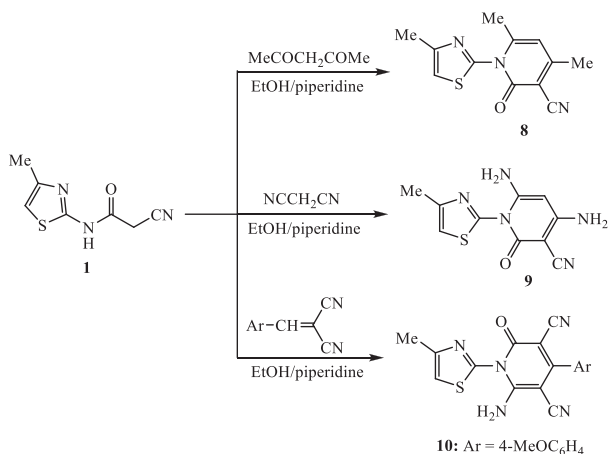
and multiplet in the region from δ 7.28 to δ 7.64 ppm for the aromatic and thiazole-C₅ protons. In addition, deshielded two singlet signals at δ 10.24 and δ 11.82 ppm were assigned for the protons of two NH groups.

Scheme 2 represents the chemical trends of thiazolyl-cyanoacetamide derivative **1** with acetylacetone, malononitrile, and 2-benzylidene-malononitrile. Thus, the reaction of **1** with acetylacetone was achieved by refluxing in ethanol containing drops of piperidine to furnish the corresponding 1-thiazol-2-yl-4,6-dimethylpyridine hybrid **8**, which was identified based on its spectral and elemental analysis. In a similar manner, heating of compound **1** with malononitrile in ethanol and 0.5 mL of piperidine furnished the 1-thiazol-2-yl-4,6-

diaminopyridone hybrid **9**, which was identified from its spectral and elemental analyses. Thus, IR spectrum of compound **9** exhibited the characteristic stretching vibrations for the amino (NH₂), nitrile (C≡N), and carbonyl (C=O) functions at 3372, 3281, and 3216; 2218; 1668 cm⁻¹, respectively. The ¹H-NMR spectrum of pyridone derivative **9** displayed singlet signal at δ 2.08 ppm attributed to the methyl protons. The proton of pyridine-C₅ resonated as singlet at δ 4.74 ppm, while the proton of thiazole-C₅ was verified at δ 7.56 ppm. The protons of the amino groups were verified as two singlet signals at δ 5.46 and δ 6.51 ppm.

Furthermore, the reaction of compound **1** with 2-(4-methoxybenzylidene) malononitrile was achieved by refluxing in ethanol containing piperidine to afford the corresponding 1-(thiazol-2-yl)-6-aminopyridone hybrid **10**. Structure proof of compound **10** was verified from its spectral and elemental analyses. The IR spectrum exhibited the characteristic absorption bands at wave numbers 3412 and 3317, 2209, and 1659 cm⁻¹, indicating the presence of the functional groups NH₂, C≡N, and C=O, respectively. The two singlet signals in ¹H-NMR spectrum of compound **10**, each integrated for three protons and resonated at δ 2.08 and δ 3.98 ppm, clearly indicated the methyl group at thiazole and the methoxy group. The aromatic protons resonated as two doublet signals at δ 7.14 and δ 7.53 ppm. The proton at the fifth position of thiazole resonated at δ 7.62 ppm while the protons of amino group was verified as singlet at δ 8.74 ppm.

Treatment of the key compound **1** with salicylaldehyde in ethanol containing piperidine under reflux for 4 h

Scheme 2. Synthesis of thiazolyl-pyridine hybrids **8**, **9**, and **10**.

furnished 2-imino-*N*-(4-methylthiazol-2-yl)-2*H*-chromene-3-carboxamide (**12**). A plausible mechanism for the reaction of **1** with salicylaldehyde is indicated in Scheme 3. The reaction starts through Knoevenagel condensation of thiazolyl-cyanoacetamide **1** (from the active methylene group) and to afford intermediate **11**, which underwent intramolecular cyclization *via* nucleophilic addition of the –OH function to the C ≡ N group promoted the formation of thiazolyl-chromene scaffold **12**. According to IR spectrum of **12**, the absorptions at 3383 and 3218 cm⁻¹ and 1686 cm⁻¹ indicated the presence of two NH and C=O functions, respectively, while disappearance of any absorption band near 2200 cm⁻¹ indicated the lack of nitrile function. The ¹H-NMR spectrum of **12** revealed signals at 2.10 ppm (singlet for three protons, CH₃), 7.29–7.83 ppm (multiplet for four aromatic protons and thiazole-H₅), 8.61 ppm (singlet for the proton of chromene-C₄), and 9.81 and 14.17 ppm for two protons of NH functions.

2-Cyano-*N*-(4-methylthiazol-2-yl)-acetamide (**1**) showed valuable reactivity toward a series of chemical reagents; it is distinguished by the presence of two active sites for electrophilic substitution reaction with aryl diazonium chlorides. The methylene function proved to be highly reactive toward diazo-coupling reaction with aryl diazonium chlorides than the thiazole C-5. Thus, diazo-coupling reaction of compound **1** with diazotized substituted anilines (*viz.*, 4-aminophenol, 4-aminoacetophenone, and 4-aminobenzoic acid) proceeded in pyridine at 0–5°C to furnish the corresponding *N*-(4-methylthiazol-2-yl)-2-aryldiazo-2-cyanoacetamide derivatives **13a–c** (Scheme 3). The chemical structure of thiazoles **13a–c** has been established because of their elemental analysis and spectral data. In the IR spectrum of **13b**, the presence of absorptions at 3287 cm⁻¹ referred to the (NH) functions, 2218 cm⁻¹ for the nitrile function (C ≡ N), and 1668 cm⁻¹ for the carbonyl group (C=O). The ¹H-NMR spectrum of **13b** displayed singlet at 2.11 ppm for three protons (thiazole-CH₃), singlet at 2.42 ppm for three protons (COCH₃), singlet at 7.60 ppm for one proton (thiazole-H₅), and two doublet signals at 7.68 and 8.06 ppm for the aromatic protons in addition to

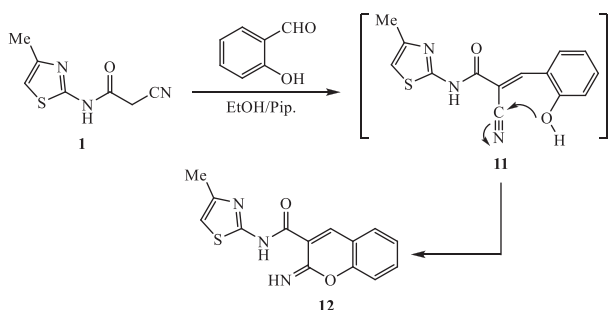
two singlet signals at 11.84 and 12.68 ppm corresponding to the protons of two (NH) functions.

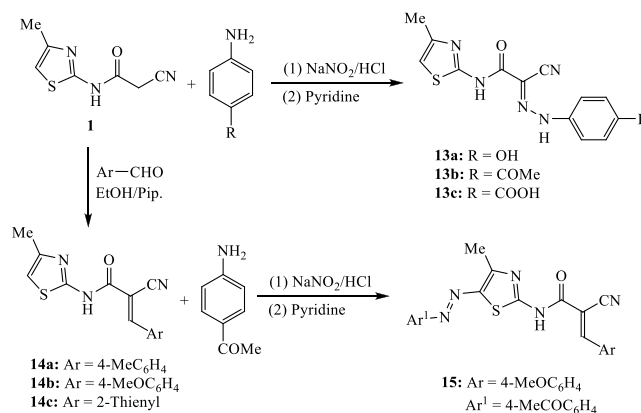
Knoevenagel condensation of cyanoacetamide **1** with various aryl/heteroaryl aldehydes (*viz.*, *p*-tolualdehyde, *p*-anisaldehyde, and thiophene-2-carbaldehyde) was proceeded by reflux in ethanol and piperidine to furnish the corresponding α,β-unsaturated nitrile derivatives **14a–c** (Scheme 4). The IR spectrum of **14b** was characterized by the presence of absorptions at 3368, 2213, and 1677 cm⁻¹ corresponding to NH, nitrile, and carbonyl functions, respectively. The ¹H-NMR of **14b** displayed singlet at 2.11 ppm for three protons (thiazole-CH₃), singlet at 3.88 ppm for three protons (OCH₃), two doublet signals at 7.02 and 7.91 ppm for the aromatic protons, and singlet for one proton at 7.61 ppm (thiazole-C₅). The two singlet signals at 8.32 and 12.26 ppm were verified the olefinic proton (CH=C) and the proton of NH, respectively.

The diazo-coupling reaction of 2-cyano-3-aryl-*N*-(4-methylthiazol-2-yl)-acrylamide derivatives **14** could not avoid the reaction at the thiazole ring. Thus, diazo-coupling reaction of **14b** with diazotized 4-aminoacetophenone furnished the corresponding 3-anisyl-2-cyano-*N*-(5-aryldiazo-thiazol-2-yl)-acrylamide derivative **15**. The diazo-coupling reaction was carried out in pyridine at 0–5°C and occurred at the active methine site (C-5) of the thiazole ring. Assignment of these products was based on its correct spectral and elemental analyses. The IR spectrum of **15** showed absorption bands at 3327, 2209, and 1670 cm⁻¹ corresponding to the imino (N-H), nitrile (C ≡ N), and carbonyl (C=O) functions, respectively. The ¹H-NMR spectrum of **15** showed singlet signal integrated for three protons at 2.27 ppm (thiazole-CH₃), singlet for three protons at 2.44 ppm (COCH₃), and singlet for three protons at 3.86 ppm (OCH₃). The aromatic protons resonated as doublet and multiplet signals in the region 7.07–7.96 ppm for the aromatic protons. The singlet signals at 8.40 and 12.38 ppm pointed to the olefinic proton (C=CH) and the proton of (NH) function, respectively.

In vitro antitumor activity. The pharmacological activities of the synthesized thiazolyl-thiazolidines **3** and **4**, thiazolyl-thiophenes **6** and **7**, thiazolyl-pyridines **8**, **9**, and **10**, and thiazolyl-chromene hybrid **12** were performed against three types of human cancer cell lines, namely, HepG2 (hepatocellular cancer), HCT-116 (colon cancer), and MCF-7 (breast cancer) using MTT colorimetric assay. Doxorubicin (DOX) was included in the experiment as the positive control cytotoxic compound for the cell lines. The IC₅₀ values were listed in Table 1 and indicated great variety in the cytotoxicity. The thiazolyl-pyridine hybrid **8** exhibited the highest cytotoxic activity with IC₅₀ values ranges from 5.12 ± 0.3 to 8.33 ± 0.6 for HepG2 and MCF-7, respectively, was very close to the value of

Scheme 3. Synthesis of thiazole-2-yl-chromene derivative **12**.



Scheme 4. Reactions of thiazolyl cyanoacetamide **1** with aryl diazonium chlorides and aromatic aldehydes.

standard drug used. The reactivity of **8** may be attributed to its chemical structure, where two function groups ($C \equiv N$ and $C=O$) present on one side of pyridine ring without any steric hindrances facilitate bonding with the receptors that was explained by molecular docking. Despite of the compound **10** that has more than one function group on the pyridine ring ($2C \equiv N$, NH_2 , and $C=O$), its cytotoxicity (9.39 ± 0.6 HCT-116 and 11.86 ± 0.7 MCF-7) was less than compound **8** that may be related to the presence of *p*-methoxybenzene in position 4 of pyridine ring. Compound **12** with the chromene substituted part was less active than compounds **8** and **10** (14.46 ± 1.1 HepG2 and 18.48 ± 1.2 HCT-116) although it is closer to

the structure of DOX. It was expected that the fused rings of compound **12** will play the same role of as DOX, where doxorubicin inhibits the progression of topoisomerase II, an enzyme which relaxes supercoils in DNA for transcription [23], and stabilizes the topoisomerase II complex after it has broken the DNA chain for replication, preventing the DNA double helix from being resealed and thereby stopping the process of replication [24].

Molecular docking. The docking experiment on 1HVY (TS) was carried out by superimposing the energy minimized ligand on the active site in the Protein Data Bank file 1HVY, after which the ligand was deleted. The method of docking calculations in MOE is the default Triangle Matcher placement along with London DG refinement. Ranking of the final poses was carried out according to the free energy of binding of the ligand using GBVI/WSA dG scoring function. For each ligand, 10 poses were selected and the ligand–enzyme complex with lowest score (binding energy) was selected.

Docking analysis. From biological data, the most antitumor active compounds over MCF-7, HCT-116, and HepG2 cell lines are compounds **8**, **10**, **12**, and DOX, and molecular docking calculations have been performed using 1HVY inhibitor binding site to elucidate its interactions with these active compounds and to predict if these compounds have analogous binding mode to the native inhibitor assuming that the active compounds **8**, **10**, **12**, and DOX might demonstrate antiproliferative action against MCF-7, HepG2, and HCT-116 cell lines through inhibition of TS as it can be seen from Table 1.

To validate of the docking procedure and accuracy, native co-crystallized ligand (raltitrexed) docking was used; raltitrexed was redocked in the same inhibitor binding site and found that is exactly superimposed on the native co-crystallized one with root-mean-square

Table 1

Cytotoxic activity of the synthesized thiazolyl-thiazolidine, thiazolyl-thiophene, thiazolyl-pyridine, and thiazolyl-chromene hybrids.

Compound	<i>In vitro</i> cytotoxicity IC ₅₀ (μg/mL)		
	HepG2	HCT-116	MCF-7
DOX	4.50 ± 0.2	5.23 ± 0.3	4.17 ± 0.2
1	33.82 ± 1.5	38.48 ± 1.8	31.43 ± 1.3
3	29.04 ± 1.3	32.37 ± 1.4	30.41 ± 0.9
4	34.61 ± 1.8	38.62 ± 1.6	32.68 ± 1.2
6	52.44 ± 2.1	48.61 ± 1.8	55.33 ± 2.0
7	42.08 ± 1.8	49.46 ± 2.1	58.71 ± 2.2
8	5.12 ± 0.3	11.45 ± 0.8	8.33 ± 0.6
9	20.21 ± 1.2	26.41 ± 1.4	28.16 ± 1.6
10	12.62 ± 1.1	9.39 ± 0.6	11.86 ± 0.7
12	14.46 ± 1.1	18.48 ± 1.2	22.52 ± 0.9
13a	67.27 ± 2.3	61.84 ± 2.4	58.55 ± 1.7
13b	54.28 ± 1.4	58.34 ± 1.8	50.36 ± 1.6
13c	71.04 ± 2.1	55.08 ± 2.4	67.43 ± 2.4
14a	34.06 ± 0.8	39.62 ± 1.1	32.12 ± 0.7
14b	23.62 ± 1.0	36.02 ± 1.2	24.73 ± 0.8
14c	41.17 ± 1.2	44.63 ± 1.5	53.27 ± 1.4
15	64.16 ± 2.6	57.46 ± 2.5	59.19 ± 2.8

IC₅₀ (μg/mL): 1–10 (very strong); 11–20 (strong); 21–50 (moderate); 51–100 (weak); above 100 (non-cytotoxic); DOX, doxorubicin.

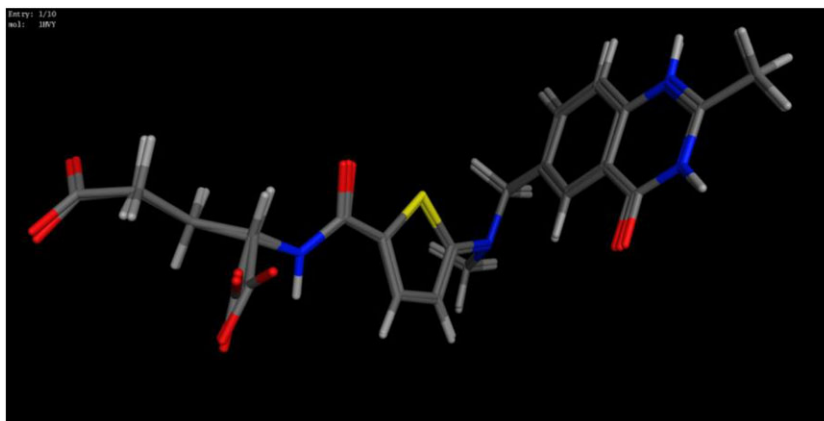


Figure 1. Re-docking of raltitrexed ligand in the (1HVV) X-ray crystal structure. The root-mean-square deviation between re-docked ligands and the corresponding X-ray crystal structure coordinates is ≤ 0.75 Å. [Color figure can be viewed at wileyonlinelibrary.com]

deviation being less than or equal to 0.75 Å (Fig. 1) and binding free energies of -37.52 kcal/mol. Hydrogen bonding network between the amino acids and the docked ligand was the same as those between the amino

acids and the native ligand compound; this demonstrate the accuracy of docking procedure.

Docking calculations performed here is carried out using MOE 2010.12 software installed on 8.0G, 64-bit, Core

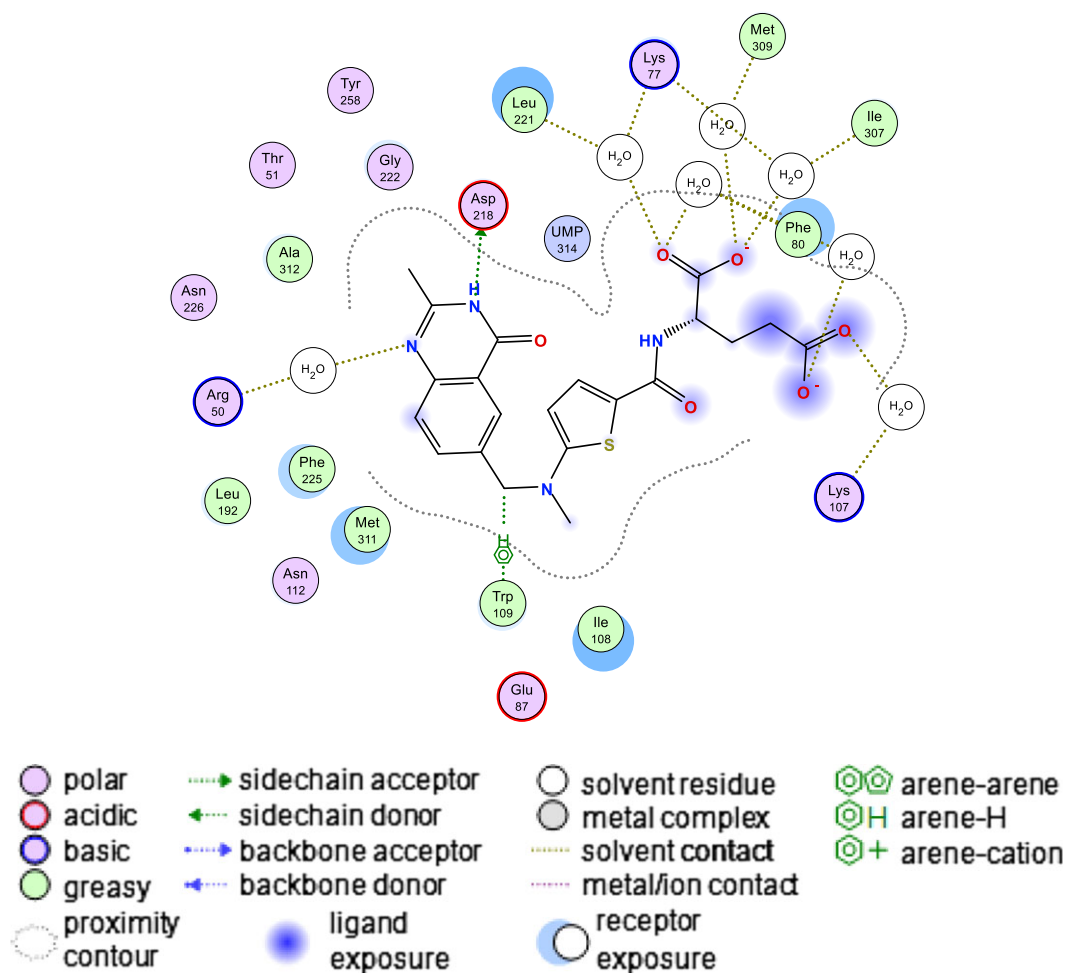


Figure 2. The interaction of the co-crystallized ligand (raltitrexed) and the binding site within the (1HVV) thymidylate synthase, seven water molecules were H-bond bridged between binding site residues and donor atoms from the co-crystallized ligand. [Color figure can be viewed at wileyonlinelibrary.com]

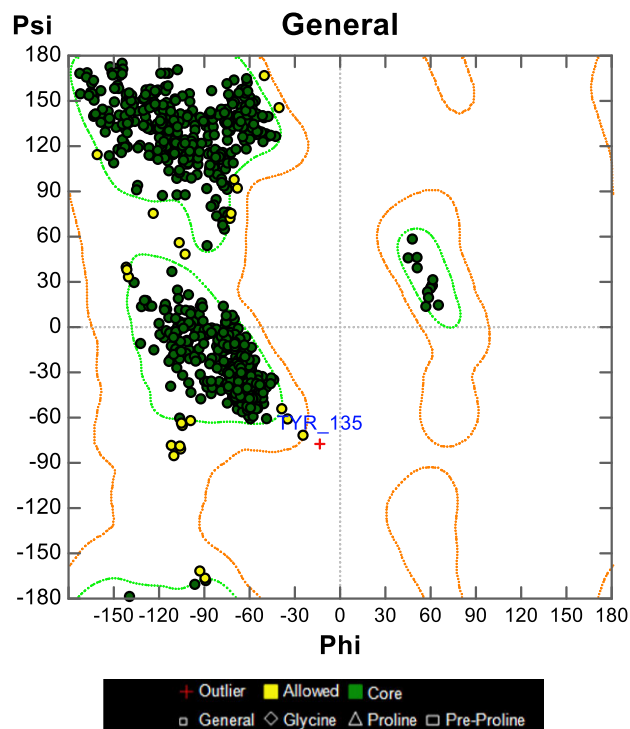


Figure 3. Ramchandran plot [(1HVY) thymidylate synthase] after energy and residue optimization, this is revealing the health of the protein. [Color figure can be viewed at wileyonlinelibrary.com]

(TM) I5. MOE 2010.12; automated docking program was used to dock ligands along with the inhibitor (raltitrexed) into inhibitor binding site. Force field MMFF94 was used to energy-minimized the complexes till to reach gradient convergence of 0.01 kcal/mol. The validation of the binding mode as per the amino acid residue predicted to be part of the binding site is shown (Fig. 2). Amino acid residues involved in the binding of protein to raltitrexed were predicted as Lys77, Leu221, Asp218, Arg50, Met309, Ile307, Lys107, and Trp109 (Fig. 3).

Binding affinity of the compounds is represented in Table 2 along with the hydrogen bond interaction with the target receptor. The compounds that give the best docking scores, according to their binding free energy and the best H-bond interactions, were compounds **8** (Fig. 4), **10** (Fig. 5), and **12** (Figs 6 and 7). Most of the synthesized compounds gave binding affinity less than the native ligand (raltitrexed) which binding free energy was -37.52 kcal/mol, while the score of binding free energy of most of the new synthesized compounds was around -10 to -19 kcal/mol. The overall correlation between binding free energy (represented as p-docking score) and the biological activity data of the synthesized compounds (represented as IC₅₀) against MCF-7, HepG2, and HCT-116 are shown in (Fig. 8). Some of the synthesized compounds' biological activities are

Table 2

Comparative docking scores, Ki values, and H-bond interaction between ligands and binding site of (1HVY) thymidylate synthase.

Molecule	Docking score (kcal/mol)	P-docking score	Ki value	H-bond interaction				RMSD Å
				Involved receptor	Atom of compound	Atom of receptor	H-bond length	
1	-10.39	1.02	2.37E-08	Asp218	CH ring	CO	1.93	1.29
					CO	NH	2.44	
3	-13.56	1.13	1.12E-10	Lys77	C=NH	NH	2.67	1.85
4	-15.22	1.18	6.78E-12	Arg50	NH	NH	1.85	1.32
5	-13.88	1.14	6.56E-11	Arg50	C=NH	NH	2.12	1.85
6	-13.32	1.12	1.69E-10	Asp218	SH	CO	3.67	1.62
7	-13.91	1.14	6.21E-11	Asp218	NH	CO	2.05	1.30
8	-18.42	1.27	3.04E-14	Arg50	CO	NH	1.99	1.08
					CN	NH	1.88	
9	-14.27	1.15	3.38E-11	Arg50	CO	NH	1.75	1.56
				Asp218	CH ring	CO	2.10	
10	-17.72	1.25	9.923E-14	Lys77	CN	NH	2.53	1.81
12	-17.39	1.248	1.73E-13	Asp218	NH	CO	1.59	1.50
13a	-12.17	1.09	1.18E-09	Arg50	CN ring	NH	1.89	0.87
13b	-12.09	1.08	1.34E-09	Lys77	CN	NH	2.38	1.19
13c	-12.59	1.10	5.78E-10	Arg50	CO	NH	1.97	1.14
14a	-13.58	1.13	1.09E-10	Arg50	CN	NH	2.37	1.11
14b	-12.98	1.11	2.98E-10	Lys77	CN	NH	2.63	1.18
14c	-12.74	1.11	4.48E-10	Arg50	CN	NH	1.90	1.07
					CN	NH	2.25	
15	-15.09	1.18	8.45E-12	Arg50	CO	NH	1.67	1.22
DOX	-19.35	1.29	6.35E-15	Asp218	NH	CO	1.75	1.87

RMSD, root-mean-square deviation.

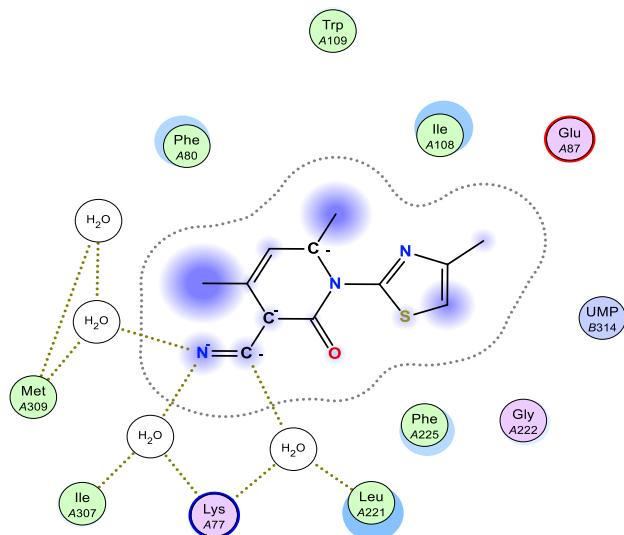


Figure 4. The interaction of the active compound **8** ligand and the binding site within the (1HVY) thymidylate synthase, four water molecules were H-bond bridged between binding site residues and donor atoms from the active compound **8**. [Color figure can be viewed at wileyonlinelibrary.com]

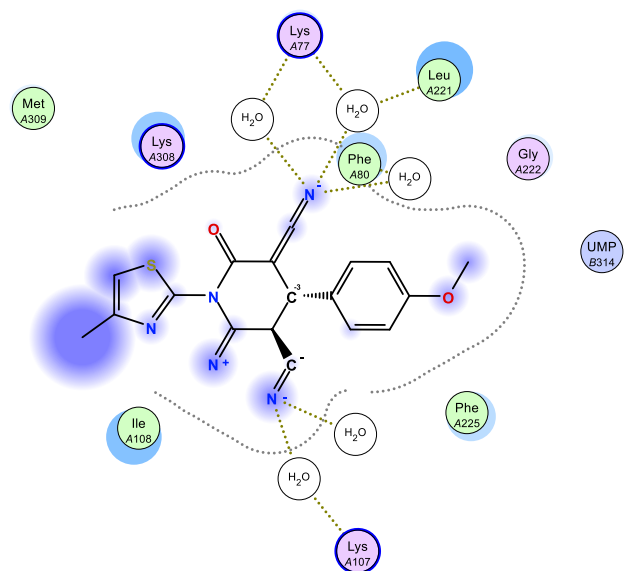


Figure 5. The interaction of the active compound **10** ligand and the binding site within the (1HVY) thymidylate synthase, four water molecules were H-bond bridged between binding site residues and donor atoms from the active compound **10**. [Color figure can be viewed at wileyonlinelibrary.com]

correlated with their binding free energy, and some are out of correlation.

EXPERIMENTAL

All melting points (uncorrected) were determined on an electrothermal Gallenkamp apparatus (Weiss-Gallenkamp,

Loughborough, UK). The IR spectra were measured on a Thermo Scientific Nicolet iS10 FTIR spectrometer (Waltham, MA). $^1\text{H-NMR}$ spectra were recorded in $\text{DMSO-}d_6$ on Bruker WP spectrometer (Rheinstetten, Germany) at 400 MHz using tetramethylsilane as an internal standard. The mass spectra were recorded on a Quadrupole GC/MS Thermo Scientific Focus/DSQII (Waltham, MA) at 70 eV. Elemental analyses (C, H, and N) were determined on Perkin-Elmer 2400 analyzer (PerkinElmer Instruments, Shelton, CT).

Synthesis of 2-cyano-2-(3-phenylthiazolidin-2-ylidene)-N-(4-methylthiazol-2-yl)-acetamide scaffolds **3 and **4**.** To a stirred suspension of 2-cyano-*N*-(4-methylthiazol-2-yl)acetamide (**1**) (5 mmol, 0.90 g) and potassium hydroxide (5 mmol, 0.28 g) in 15 mL of DMF, phenyl isothiocyanate (5 mmol, 0.6 mL) was added, and the reaction mixture was allowed to stir at an ambient temperature for 4 h. After which, 5 mmol of the appropriate α -chlorinated reagent (viz., ethyl chloroacetate and chloroacetonitrile) was added, and the stirring was continued for additional 4 h. The solid that formed by pouring the reaction mixture onto ice water has been collected by filtration. The crude product was purified by recrystallization from ethyl alcohol.

2-Cyano-*N*-(4-methylthiazol-2-yl)-2-(4-oxo-3-phenylthiazolidin-2-ylidene)-acetamide (3**).** Yellow powder, yield 62%; m.p. 192–194°C. IR (KBr): $\nu_{\text{max}}/\text{cm}^{-1}$ = 3127 (N-H), 2199 (C \equiv N), 1740 (C=O). $^1\text{H-NMR}$ ($\text{DMSO-}d_6$) δ /ppm: 2.11 (s, 3H, CH_3), 4.04 (s, 2H, CH_2), 7.32–7.51 (m, 5H, Ar-H), 7.58 (s, 1H, thiazole- H_5), 11.88 (s, 1H, NH). *Anal.* Calcd for $\text{C}_{16}\text{H}_{12}\text{N}_4\text{O}_2\text{S}_2$ (356): C, 53.92; H, 3.39; N, 15.72%. Found: C, 53.71; H, 3.46; N, 15.81%.

2-Cyano-2-(4-imino-3-phenylthiazolidin-2-ylidene)-*N*-(4-methylthiazol-2-yl)-acetamide (4**).** Yellow powder, yield 48%, m.p. 166–167°C. IR (KBr): $\nu_{\text{max}}/\text{cm}^{-1}$ = broad at 3346 (N-H), 2194 (C \equiv N), 1664 (C=O). $^1\text{H-NMR}$ ($\text{DMSO-}d_6$) δ /ppm: 2.12 (s, 3H, CH_3), 3.92 (s, 2H, CH_2), 7.05–7.48 (m, 5H, Ar-H), 7.56 (s, 1H, thiazole- H_5), 9.82 (s, 1H, NH), 12.04 (s, 1H, NH). *Anal.* Calcd for $\text{C}_{16}\text{H}_{13}\text{N}_5\text{OS}_2$ (355): C, 54.07; H, 3.69; N, 19.70%. Found: C, 54.21; H, 3.76; N, 19.58%.

Synthesis of 2-cyano-3-mercapto-3-(phenylamino)-*N*-(4-methylthiazol-2-yl)-acrylamide (5**).** To a stirred suspension of cyanoacetamide scaffold **1** (10 mmol, 1.81 g) and potassium hydroxide (10 mmol, 0.56 g) in 25 mL of DMF, phenyl isothiocyanate (10 mmol, 1.2 mL) was dropwise added and permitted to stir at an ambient temperature for 4 h. After which, the reaction mixture was poured onto ice water and neutralized by diluted HCl. The solid formed has been collected up by filtration and recrystallized by heating in ethyl alcohol.

Yellow powder, yield 76%, m.p. 166–168°C. IR (KBr): $\nu_{\text{max}}/\text{cm}^{-1}$ = 3314, 3196 (N-H), 2182 (C \equiv N), 1659

(C=O). $^1\text{H-NMR}$ (DMSO- d_6) δ/ppm : 2.08 (s, 3H, CH_3), 2.72 (s, 1H, SH), 7.05–7.45 (m, 5H, Ar-H), 7.58 (d, 1H, thiazole- H_5), 10.28 (s, 1H, NH), 11.94 (s, 1H, NH). *Anal.* Calcd for $\text{C}_{14}\text{H}_{12}\text{N}_4\text{OS}_2$ (316): C, 53.36; H, 3.90; N, 17.71%. Found: C, 53.14; H, 3.82; N, 17.83%.

Synthesis of 5-substituted-4-amino-2-(phenylamino)-*N*-(4-methylthiazol-2-yl)-thiophene-3-carboxamide scaffolds 6 and 7. To a solution of thiocarbamoyl scaffold 5 (2 mmol, 0.63 g) in 15 mL of ethanol, the appropriate α -chlorinated reagent (viz., ethyl chloroacetate and chloroacetonitrile, 2 mmol) and 0.5 mL of $(\text{C}_2\text{H}_5)_3\text{N}$ were added, and the reaction mixture was refluxed for 2 h, after which left to cool to 25°C. The solid formed was filtered off and dried to afford the thiophene scaffolds 6 and 7.

Ethyl 4-(4-methylthiazol-2-ylcarbamoyl)-3-amino-5-(phenylamino)thiophene-2-carboxylate (6). Yellow powder, yield 64%, m.p. 220–221°C. IR (KBr): $\nu_{\text{max.}}/\text{cm}^{-1}$ = 3416, 3243 (N-H stretch of NH_2 and NH), broad at 1638 (C=O). $^1\text{H-NMR}$ (DMSO- d_6) δ/ppm : 1.31 (t, J = 7.1 Hz, 3H, CH_3), 2.11 (s, 3H, CH_3), 4.30 (q, J = 7.2 Hz, 2H, CH_2), 6.90 (s, 2H, NH_2), 7.28–7.64 (m, 6H, Ar-H and thiazole- H_5), 10.24 (s, 1H, NH), 11.82 (s, 1H, NH). *Anal.* Calcd for $\text{C}_{18}\text{H}_{18}\text{N}_4\text{O}_3\text{S}_2$ (402): C, 53.71; H, 4.51; N, 13.92%. Found: C, 53.86; H, 4.57; N, 13.83%.

4-Amino-5-cyano-2-(phenylamino)-*N*-(4-methylthiazol-2-yl)thiophene-3-carboxamide (7). Yellowish brown powder, yield 72%, m.p. 213–215°C. IR (KBr): $\nu_{\text{max.}}/\text{cm}^{-1}$ = 3416, 3220, 3175 (N-H stretch of NH_2 and NH), 2172 ($\text{C} \equiv \text{N}$), shoulder near 1633 (C=O). $^1\text{H-NMR}$ (DMSO- d_6) δ/ppm : 2.11 (s, 3H, CH_3), 6.62 (s, 2H, NH_2), 7.21–7.61 (m, 6H, Ar-H and thiazole- H_5), 10.41 (s, 1H,

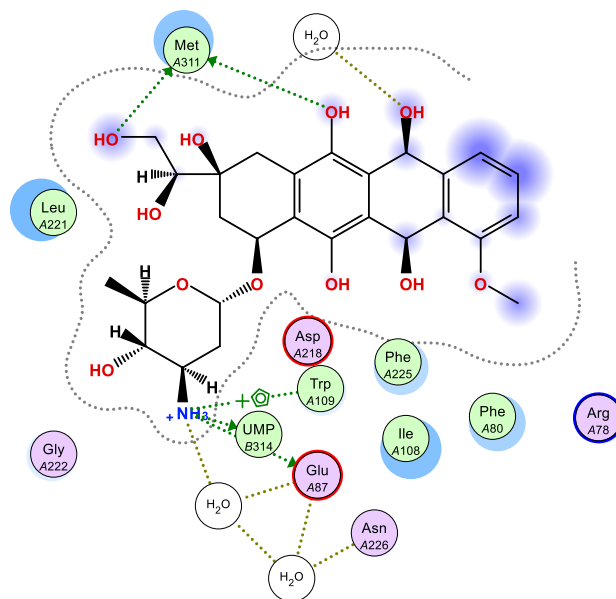


Figure 7. The interaction of the active compound doxorubicin ligand and the binding site within the (1HYV) thymidylate synthase, four water molecules were H-bond bridged between binding site residues and donor atoms from the active compound doxorubicin. [Color figure can be viewed at wileyonlinelibrary.com]

NH), 12.04 (s, 1H, NH). *Anal.* Calcd for $\text{C}_{16}\text{H}_{13}\text{N}_5\text{OS}_2$ (355): C, 54.07; H, 3.69; N, 19.70%. Found: C, 54.19; H, 3.65; N, 19.62%.

Synthesis of 4,6-disubstituted-2-oxo-1-(4-methylthiazol-2-yl)-1,2-dihydro pyridine-3-carbonitriles 8 and 9. A solution of cyanoacetamide scaffold 1 (4 mmol, 0.72 g) and acetylacetone or malononitrile (4 mmol) in 20 mL of

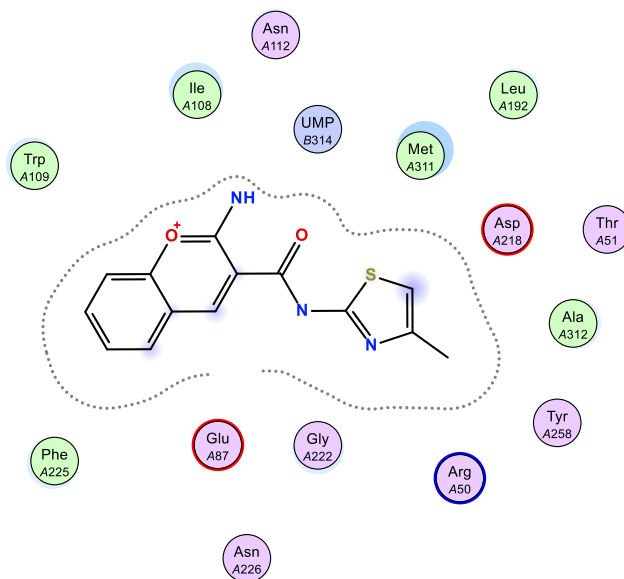


Figure 6. The interaction of the active compound 12 ligand and the binding site within the (1HYV) thymidylate synthase, four water molecules were H-bond bridged between binding site residues and donor atoms from the active compound 12. [Color figure can be viewed at wileyonlinelibrary.com]

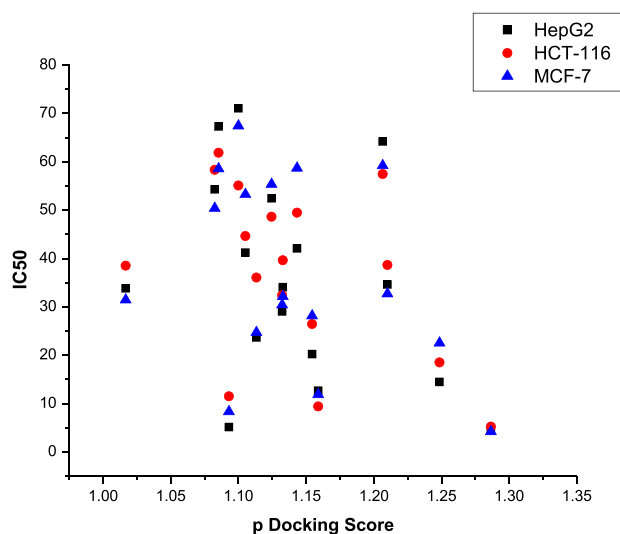


Figure 8. The correlation between IC₅₀ (µg/mL) enzymatic inhibition and the Molecular Operating Environment p-docking score. [Color figure can be viewed at wileyonlinelibrary.com]

EtOH containing 0.5 mL of piperidine was heated under reflux for 6 h. After which, the reaction mixture was cooled to 25°C and the solid formed was collected by filtration. Recrystallization was carried out from dioxane to afford the pyridine derivatives **8** and **9**, respectively.

4,6-Dimethyl-2-oxo-1-(4-methylthiazol-2-yl)-1,2-dihydropyridine-3-carbonitrile (8). Yellowish white crystals, yield 69%, m.p. 242–244°C. IR (KBr): $\nu_{\max.}/\text{cm}^{-1} = 2222$ (C \equiv N), 1674 (C=O). ¹H-NMR (DMSO-*d*₆) δ/ppm : 2.08 (s, 3H, CH₃), 2.39 (s, 3H, CH₃), 2.40 (s, 3H, CH₃), 6.49 (s, 1H, pyridine-H₅), 7.57 (s, 1H, thiazole-H₅). *Anal.* Calcd for C₁₂H₁₁N₃OS (245): C, 58.76; H, 4.52; N, 17.13%. Found: C, 58.92; H, 4.45; N, 17.24%.

4,6-Diamino-1-(4-methylthiazol-2-yl)-2-oxo-1,2-dihydropyridine-3-carbonitrile (9). Brown powder, yield 69%, m.p. 192–193°C. IR (KBr): $\nu_{\max.}/\text{cm}^{-1} = 3372$, 3281, 3216 (NH₂), 2218 (C \equiv N), 1668 (C=O). ¹H-NMR (DMSO-*d*₆) δ/ppm : 2.08 (s, 3H, CH₃), 4.74 (s, 1H, pyridine-H₅), 5.46 (s, 2H, NH₂), 6.51 (s, 2H, NH₂), 7.56 (s, 1H, thiazole-H₅). *Anal.* Calcd for C₁₀H₉N₅OS (247): C, 48.57; H, 3.67; N, 28.32%. Found: C, 48.34; H, 3.60; N, 28.44%.

Synthesis of 6-amino-4-(4-anisyl)-1,2-dihydro-2-oxo-1-(4-methylthiazol-2-yl)pyridine-3,5-dicarbonitrile 10. To a solution of cyanoacetamide scaffold **1** (4 mmol, 0.72 g) and 2-(4-methoxybenzylidene) malononitrile (4 mmol, 0.74 g) in 20 mL of ethanol, five drops of piperidine were dropwise added. After which, the reaction mixture was boiled under reflux for 2 h, and the solid product was filtered off to give the desired pyridine derivative **10**.

Brown crystals, yield 69%, m.p. 275–277°C. IR (KBr): $\nu_{\max.}/\text{cm}^{-1} = 3412$, 3317 (NH₂), 2209 (C \equiv N), 1659

(C=O). ¹H-NMR (DMSO-*d*₆) δ/ppm : 2.08 (s, 3H, CH₃), 3.86 (s, 3H, OCH₃), 7.14 (d, *J* = 8.8 Hz, 2H, Ar-H), 7.53 (d, *J* = 8.8 Hz, 2H, Ar-H), 7.62 (s, 1H, thiazole-H₅), 8.74 (s, 2H, NH₂). *Anal.* Calcd for C₁₈H₁₃N₅O₂S (363): C, 59.49; H, 3.61; N, 19.27%. Found: C, 59.58; H, 3.65; N, 19.35%.

Synthesis of 2-imino-N-(4-methylthiazol-2-yl)-2H-chromene-3-carboxamide (12). A suspension of cyanoacetamide scaffold **1** (4 mmol, 0.72 g) and salicylaldehyde (4 mmol, 0.42 mL) was refluxed for 4 h in 15 mL of EtOH containing 0.5 mL of piperidine. After which, the reaction mixture was cooled to room temperature, and the solid formed was collected by filtration. Recrystallization of the product has been achieved by heating in ethyl alcohol.

Yellow crystals, yield 64%, m.p. 132–134°C. IR (KBr): $\nu_{\max.}/\text{cm}^{-1} = 3383$, 3218 (N-H), 1686 (C=O). ¹H-NMR (DMSO-*d*₆) δ/ppm : 2.10 (s, 3H, CH₃), 7.29–7.83 (m, 5H, Ar-H, thiazole-H₅), 8.61 (s, 1H, chromene-H₄), 9.81 (s, 1H, NH), 14.17 (s, 1H, NH). *Anal.* Calcd for C₁₄H₁₁N₃O₂S (285): Calcd: C, 58.94; H, 3.89; N, 14.73%. Found: C, 58.82; H, 3.96; N, 14.81%.

Synthesis N-aryl-2-((4-methylthiazol-2-yl)amino)-2-oxoacetohydrazonoyl cyanide 13a–c. To a cold solution of the cyanoacetamide scaffold **1** (5 mmol, 0.90 g) in pyridine (20 mL), the appropriate diazonium salt of the appropriate aromatic amine (4-hydroxy-aniline, 4-aminoacetophenone, and 4-aminobenzoic acid) (5 mmol) was added. The addition was carried out portion wise with stirring at 0–5°C over a period of 30 min. After complete addition, the reaction mixture was kept in an ice bath for 12 h and finally diluted with water. The solid that formed was filtrated, washed with water, dried, and finally recrystallized from the EtOH/EMF mixture (2:1) to afford the corresponding hydrazonoyl cyanides **13a–c**.

N-(4-Hydroxyphenyl)-2-((4-methylthiazol-2-yl)amino)-2-oxoacetohydrazonoyl cyanide (13a). Orange crystals, yield 69%, m.p. 271–273°C. IR (KBr): $\nu_{\max.}/\text{cm}^{-1} = 3241$ (O-H), 3173 (N-H), 2216 (C \equiv N), 1664 (C=O). ¹H-NMR (DMSO-*d*₆) δ/ppm : 2.10 (s, 3H, CH₃), 7.14 (d, 2H, Ar-H), 7.44 (d, 2H, Ar-H), 7.62 (s, 1H, thiazole-H₅), 9.54 (s, 1H, OH), 11.58 (s, 1H, NH), 12.63 (s, 1H, NH). *Anal.* Calcd for C₁₃H₁₁N₅O₂S (301): C, 51.82; H, 3.68; N, 23.24%. Found: C, 51.96; H, 3.62; N, 23.34%.

N-(4-Acetylphenyl)-2-((4-methylthiazol-2-yl)amino)-2-oxoacetohydrazonoyl cyanide (13b). Red crystals, yield 74%; m.p. 264–266°C. IR (KBr): $\nu_{\max.}/\text{cm}^{-1} = 3287$ (N-H), 2218 (C \equiv N), broad at 1668 (C=O). ¹H-NMR (DMSO-*d*₆) δ/ppm : 2.11 (s, 3H, CH₃), 2.42 (s, 3H, CH₃), 7.60 (s, 1H, thiazole-H₅), 7.68 (d, 2H, Ar-H), 8.06 (d, 2H, Ar-H), 11.84 (s, 1H, NH), 12.68 (s, 1H, NH). *Anal.* Calcd for C₁₅H₁₃N₅O₂S (327): C, 55.03; H, 4.00; N, 21.39%. Found: C, 55.19; H, 4.04; N, 21.28%.

***N*-(4-Carboxyphenyl)-2-((4-methylthiazol-2-yl)amino)-2-oxoacetohydrazonoyl cyanide (13c).** Red crystals, yield 58%, m.p. 255–256°C. IR (KBr): $\nu_{\max}/\text{cm}^{-1}$ = 3276, (N-H), 2748 (O-H), 2220 (C \equiv N), broad at 1678 (C=O). $^1\text{H-NMR}$ (DMSO- d_6) δ/ppm : 2.10 (s, 3H, CH₃), 7.64 (s, 1H, thiazole-H₅), 7.72 (d, 2H, Ar-H), 8.15 (d, 2H, Ar-H), 11.73 (s, 1H, NH), 12.63 (s, 1H, OH), 12.91 (s, 1H, NH). *Anal.* Calcd for C₁₄H₁₁N₅O₃S (329): C, 51.06; H, 3.37; N, 21.27%. Found: C, 50.93; H, 3.40; N, 21.20%.

Synthesis of 3-aryl-2-cyano-*N*-(4-methylthiazol-2-yl)acrylamides 14a-c. To a solution of the cyanoacetamide **1** (5 mmol, 0.90 g) and the appropriate aromatic aldehydes (4-methylbenzaldehyde, 4-methoxybenzaldehyde, and thiophene-2-carbaldehyde) (5 mmol) in dioxane (20 mL), five drops of piperidine was added, and the reaction mixture was refluxed for 4 h. The solid that formed was filtered off, dried, and finally recrystallized from dioxane.

2-Cyano-*N*-(4-methylthiazol-2-yl)-3-(4-tolyl)acrylamide (14a). Yellow crystals, yield 82%; m.p. 235–238°C. IR (KBr): $\nu_{\max}/\text{cm}^{-1}$ = 3337 (N-H), 2216 (C \equiv N), 1675 (C=O). $^1\text{H-NMR}$ (DMSO- d_6) δ/ppm : 2.12 (s, 3H, CH₃), 2.40 (s, 3H, CH₃), 7.42 (d, 2H, Ar-H), 7.55 (s, 1H, thiazole-H₅), 7.83 (d, 2H, Ar-H), 8.38 (s, 1H, CH=C), 12.28 (s, 1H, NH). *Anal.* Calcd for C₁₅H₁₃N₃OS (283): C, 63.58; H, 4.62; N, 14.83%. Found: C, 63.46; H, 4.66; N, 14.75%.

3-(4-Anisyl)-2-cyano-*N*-(4-methylthiazol-2-yl)acrylamide (14b). Yellow crystals, yield 73%, m.p. 230–233°C. IR (KBr): $\nu_{\max}/\text{cm}^{-1}$ = 3368 (N-H), 2213 (C \equiv N), 1677 (C=O). $^1\text{H-NMR}$ (DMSO- d_6) δ/ppm : 2.11 (s, 3H, CH₃), 3.88 (s, 3H, OCH₃), 7.02 (d, 2H, Ar-H), 7.61 (s, 1H, thiazole-H₅), 7.91 (d, 2H, Ar-H), 8.32 (s, 1H, CH=C), 12.26 (s, 1H, NH). *Anal.* Calcd for C₁₅H₁₃N₃O₂S (299): C, 60.18; H, 4.38; N, 14.04%. Found: C, 60.26; H, 4.34; N, 14.10%.

2-Cyano-*N*-(4-methylthiazol-2-yl)-3-(2-thienyl)acrylamide (14c). Yellow crystals, yield 65%, m.p. 240–242°C. IR (KBr): $\nu_{\max}/\text{cm}^{-1}$ = 3307 (N-H), 2221 (C \equiv N), 1674 (C=O). $^1\text{H-NMR}$ (DMSO- d_6) δ/ppm : 2.12 (s, 3H, CH₃), 7.28 (m, 1H, thiophene-H₄), 7.64 (s, 1H, thiazole-H₅), 7.65 (d, 1H, thiophene-H₃), 8.15 (d, 1H, thiophene-H₅), 8.44 (s, 1H, CH=C), 12.53 (s, 1H, NH). *Anal.* Calcd for C₁₂H₉N₃O₂S (275): C, 52.34; H, 3.29; N, 15.26%. Found: C, 52.18; H, 3.22; N, 15.37%.

Synthesis of *N*-(5-(4-acetylphenylazo)-4-methylthiazol-2-yl)-2-cyano-3-(4-methoxy phenyl)acrylamide (15). To a cold solution of **14b** (5 mmol, 1.50 g) in pyridine (20 mL), the diazonium salt derived from 4-aminoacetophenone (5 mmol, 0.68 g) was added. The addition was carried out portion wise with stirring at 0–5°C over a period of 30 min. After complete addition, the reaction mixture was kept in an ice chest overnight and finally diluted with water. The solid that formed was

collected by filtration, washed with water, dried, and finally recrystallized from dioxane.

Brown powder, yield 56%, m.p. 274–276°C. IR (KBr): $\nu_{\max}/\text{cm}^{-1}$ = 3327 (N-H), 2209 (C \equiv N), broad at 1670 (C=O). $^1\text{H-NMR}$ (DMSO- d_6) δ/ppm : 2.27 (s, 3H, CH₃), 2.44 (s, 3H, CH₃), 3.86 (s, 3H, OCH₃), 7.07 (d, 2H, Ar-H), 7.46–7.96 (m, 6H, Ar-H), 8.25 (s, 1H, CH=C), 12.38 (s, 1H, NH). *Anal.* Calcd for C₂₃H₁₉N₅O₃S (445): C, 62.01; H, 4.30; N, 15.72%. Found: C, 62.20; H, 4.22; N, 15.60%.

Anticancer screening. For the estimation of the cytotoxicity effects of the investigated thiazole-containing heterocycles derived from *N*-(4-methylthiazol-2-yl)-cyanoacetamide, three human cancer cell lines were used (viz., hepatocellular cancer HepG-2, colon cancer HCT-116, and breast cancer MCF-7). These cell lines were obtained from ATCC *via* holding company for biological products and vaccines (VACSERA), Cairo, Egypt. Cytotoxicity determinations are based the transformation of the yellow 3-(4,5-dimethylthiazol-2-yl)-2,5-diphenyl tetrazolium bromide (MTT) to a purple formazan derivative by mitochondrial succinate dehydrogenase in practical cells. The method of this MTT assay was performed as previously described in detail [25–28].

Molecular docking study. Docking calculations carried out here were performed on (Intel Core I5) Toshiba Satellite with running Windows 10, installed MOE software version 2010.12, respectfully available from CCG (Chemical Computing Group Inc.), 1010 Sherbrooke Street West, Suite 910, Montreal, QC [29].

Selection of crystal structures of the protein. Crystallographic structure of the ligand bound of our target protein (TS) is downloaded from the Protein Data Bank website (<https://www.rcsb.org>). In this study, 1HVY crystal structure have been selected and evaluated for docking. Furthermore, errors of the protein structure were corrected using MOE structure preparation process. Initially, and for generation of suitable protein structure for docking the hydrogen atoms were assigned, water molecules contained in the protein structure with distance further than 10 Å were removed, partial charges were assigned, and energy of the remaining structure was minimized using the default parameters of MOE energy minimization algorithm (gradient: 0.01, Force field: MMFF94X). This is performed based on default rules (Temperature of the system is 300 K, pH is 7.0, and dielectric constant is 1.0). Finally, collection of residues within distance of 6.5 Å from the bound co-crystallographic inhibitor was used to define the active site of the protein.

Preparation of the ligand for docking. Molecular Operating Environment (MOE) builder tool is used in building the ligand structure, followed by correction of atom types, including hybridization states, and defining of the bond types, then addition of hydrogen atoms, assigning

of atom charges, and then, the structures were subject to energy minimization using MMFF94x method until a gradient of 0.01 kcal/mol is reached; this process is applied for co-crystallographic ligand and synthesized ligands.

CONCLUSION

A series of thiazole derivatives contains thiazolidine, thiophene, pyridine, or chromene was synthesized, and the structures were confirmed by spectral and elemental analysis. The antiproliferative activity of the new heterocyclic compounds was screened *in vitro* against cell lines of hepatocellular cancer (HepG-2), colon cancer (HCT-116), and breast cancer (MCF-7). The most effective compounds were pyridine derivatives **8**, **10**, and the fused chromene structure **12** compared by the reference drug (doxorubicin) which is used in this study. The molecular docking was helpful in illustrating the interaction mode between the active compounds and the target protein (thymidylate thynsase in this case); hydrogen bonding network have been investigated and found that the most attractive residues that bind effectively with active compounds are Asp218, Arg50, Met309, Ile307, Lys107, and Trp109.

REFERENCES AND NOTES

- [1] Jain, A. K.; Vaidya, A.; Ravichandran, V.; Kashaw, S. K.; Agrawal, R. K. *Bioorg Med Chem* 2012, 20, 3378.
- [2] Abdel Hafez, N. A.; Elsayed, M. A.; El-Shahawi, M. M.; Awad, G. E. A.; Ali, K. A. *J Heterocyclic Chem* 2018, 55, 685.
- [3] Amin, K. M.; Kamel, M. M.; Anwar, M. M.; Khedr, M.; Syam, Y. N. *Eur J Med Chem* 2010, 45, 2117.
- [4] Turan-Zitouni, G.; Kaplancikli, Z. A.; Ozdemir, A. *Eur J Med Chem* 2010, 45, 2085.
- [5] Gundlewad, G. B.; Patil, B. R. *J Heterocyclic Chem* 2018 early view, <https://doi.org/10.1002/jhet.3098>, 55, 769.
- [6] Kaur, H.; Kumar, S.; Vishwakarma, P.; Sharma, M.; Saxena, K. K.; Kumar, A. *Eur J Med Chem* 2010, 45, 2777.
- [7] Agarwal, A.; Lata, S.; Saxena, K. K.; Srivastava, V. K.; Kumar, A. *Eur J Med Chem* 2006, 41, 1223.
- [8] Wang, S.; Zhao, Y.; Zhang, G.; Lv, Y.; Zhang, N.; Gong, P. *Eur J Med Chem* 2011, 46, 3509.
- [9] Kamel, M. M.; Ali, H. I.; Anwar, M. M.; Mohamed, N. A.; Soliman, A. M. *Eur J Med Chem* 2010, 45, 572.
- [10] Havrylyuk, D.; Mosula, L.; Zimenkovsky, B.; Vasylenko, O.; Gzella, A.; Lesyk, R. *Eur J Med Chem* 2010, 45, 5012.
- [11] Pansare, D. N.; Shelke, R. N.; Shinde, D. B. *J Heterocyclic Chem* 2017, 54, 3077.
- [12] Laine, L.; Kivitz, A. J.; Bello, A. E.; Grahm, A. Y.; Schiff, M. H.; Taha, A. S. *Am J Gastroenterol* 2012, 107, 379.
- [13] Howard, J. M.; Chremos, A. N.; Collen, M. J.; Mearthur, K. E.; Cherner, J. A.; Maton, P. N.; Ciarleglio, C. A.; Cornelius, M. J.; Gardner, J. D.; Jensen, R. T. *Gastroenterology* 1985, 88, 1026.
- [14] Borelli, C.; Schaller, M.; Niewerth, M.; Nocker, K.; Baasner, B.; Berg, D.; Tiemann, R.; Tietjen, K.; Fugmann, B.; Lang-Fugmann, S.; Korting, H. C. *Chemotherapy* 2008, 54, 245.
- [15] Guay, D. R. P. *Clin Ther* 2002, 24, 473.
- [16] Yapati, H.; Devineni, S. R.; Chirumamilla, S.; Kalluru, S. *J Chem Sci* 2016, 128, 43.
- [17] Shubakara, K.; Umesha, K. B.; Srikantamurthy, N.; Chethan, J. *J Chem Sci* 2014, 126, 1913.
- [18] Brandt, D. S.; Chu, E. *Oncol Res* 1997, 9, 403.
- [19] Chu, E.; Allegra, C. *Antifolates*; In *Cancer Chemotherapy* Chabner, B.; Collins, J. Eds.; Lippincott-Raven: Philadelphia, PA, 1996, pp. 109–148.
- [20] Heidelberger, C.; Chaundhuri, N.; Danenberg, P. *Nature* 1957, 179, 663.
- [21] Rose, M. G.; Farrell, M. P.; Schmitz, J. C. *Clin Colorectal Cancer* 2002, 1, 220.
- [22] Walker, G. N. US patent 4,435,407 1984.
- [23] Pommier, Y.; Leo, E.; Zhang, H.; Marchand, C. *Chem Biol* 2010, 17, 421.
- [24] Tacar, O.; Sriamornsak, P.; Dass, C. R. *J Pharm Pharmacol* 2013, 65, 157.
- [25] Mosmann, T. *J Immunol Methods* 1983, 65, 55.
- [26] Mauceri, H. J.; Hanna, N. N.; Beckett, M. A.; Gorski, D. H.; Staba, M.-J.; Stellato, K. A.; Bigelow, K.; Heimann, R.; Gately, S.; Dhanabalk, M.; Soff, G. A.; Sukhatmek, V. P.; Kufe, D. W.; Weichselbaum, R. R. *Nature* 1998, 394, 287.
- [27] Wang, H.; Zheng, J.; Xu, W.; Chen, C.; Wei, D.; Ni, W.; Pan, Y. *Molecules* 2017, 22, 1635.
- [28] Abd ElMonaem, H.; Abdel-Aziz, N.; Morsy, M.; Badria, F.; ElSenduny, F.; El-Ashmawy, M.; Moustafa, M. *J Appl Pharmaceutical Sci* 2018, 8, 075.
- [29] Molecular Operating Environment (MOE) 2010.12, Chemical Computing Group Inc., Quebec, Canada, 2008.